

THE EFFECTS OF ANNEALING ON MICROSTRUCTURAL CHANGES FOR
ALUMINIUM NITRIDE EPITAXIAL GROWN ON SAPPHIRE BY
TRANSMISSION ELECTRON MICROSCOPY

JESBAINS KAUR

A thesis submitted in fulfilment of the
requirements for the award of degree of
Doctor of Philosophy

Malaysia-Japan International Institute of Technology
Universiti Teknologi Malaysia

APRIL 2017

DEDICATION

To my lovely mother, who gave me endless love, trust, constant encouragement over the years, and for her prayers

To my spouse, for being very understanding and supportive in keeping me going, enduring the ups and downs during the completion of this thesis.

To my family, for their patience, support, love and prayers

This thesis is dedicated to them.

ACKNOWLEDGEMENT

I wish to express my deepest appreciation to all those who helped me, in one way or another, to complete this thesis. First and foremost I thank Waheguru, God almighty who provided me with strength, direction and showered me with blessings throughout. My sincerest gratitude to my supervisor Professor Dr. Noriyuki Kuwano for his continuous guidance and support. With his expert guidance and immense knowledge I was able to overcome all the obstacles that I encountered during my journey of Ph.D. I could not have imagine having a better advisor and mentor who has been more like a fatherly figure to me. I am very thankful to Malaysia Japan International Institute of Technology (MJIT), UTM for providing me scholarship and financing my studies. I never had to worry about any financial issue and manage to focus only on my research and publications. Also MJIT has sponsored me for Joint Supervision Programme at Kyushu University, Japan. During my stay in Japan, Prof Matsumura, Prof Tomokiyo, Tanaka Sensei, Shinano Sensei and Takayama San have helped me a lot in terms of sharing their knowledge and experience and made me feel like home. They gave me access to use High Voltage Electron Microscopy (HVEM) Lab and research facilities.

I would also like to thank my co-supervisor Dr Muhammad Rijal for his advice and support in every form he could give. Special thanks to all the members of Nano3 i-kohza, Dr Anthony, Ms Marina Lias, Mr Hamid and Ms Sarah for the stimulating weekly Rinkoh sessions, for the sleepless nights completing work to meet deadlines, supporting each other and having fun at the same time. Last but not least, the man who encouraged me to start this journey my dearest husband Mr Dilmindar Singh. He has always being so tolerant, sacrificing everything for me to keep fighting this journey. His endless love and care made me stronger to overcome hurdles in life. My upmost gratitude to my family: mother, in-laws, brothers and sisters for supporting me spiritually in this journey.

ABSTRACT

The performance of semiconductor devices depends strongly upon the microstructure of the materials. Therefore the microstructural control is intrinsically important for fabrication of high performance devices. In this research, the microstructures have been analysed in detail and the mechanisms of microstructural changes in aluminium nitride (AlN) epitaxial have been clarified for the establishment of the growth method. AlN heteroepitaxial layers were made by growing an AlN buffer layer on a (0001) sapphire substrate by the Metal Organic Vapor Phase Epitaxy (MOVPE) growth process. Annealing treatments were added before and after the deposition of an AlN buffer layer. The surface roughness of AlN was observed with an Atomic Force Microscope (AFM) and X-ray Rocking Curve (XRC). The cross section of AlN heteroepitaxial was observed by using Transmission Electron Microscope (TEM) at 200 Kv and High-Angle Annular Dark-Field (HAADF) images were observed with a Scanning Transmission Electron Microscope (STEM) at 300 kV. Thin foil specimens or lamella for the TEM observation were made using a Focused Ion Beam (FIB) mill with accelerating voltage of 15 kV~3 kV for a smooth finishing of lamella. Prior to the deposition of a medium temperature MT-AlN layer, the sapphire substrate was cleaned or pre-annealed at a high temperature, T_{An} under the atmosphere of H_2 . For annealing temperature, T_{An} less than $1250^\circ C$, the crystallinity improved but twisting domains appeared above the temperature. Threading dislocations (TDs) of type c and type-a+c with 10^8 cm^{-2} dislocation density was observed. However when the temperature was increased to $1350^\circ C$, threading dislocation were reduced. On the other hand, post deposition annealing at a high temperature between $1500^\circ C$ and $1700^\circ C$ for 2 hours under the atmosphere of N_2+CO was carried out. Cross sectional TEM revealed that after annealing at $1500^\circ C$, cone-shaped domains and threading dislocations remained. The morphology of domains and the changes in TEM image contrast strongly suggest that the domains are inversion domains. TDs of type-a and type- a+c were visible for $g = 01-10$ under the two beam condition. However, after annealing at $1550^\circ C$, the cone shaped domains coalesced with each other to leave a single domain boundary running in a zigzag laterally at the center of AlN buffer layer that the upper layer has the Al- polarity while the lower layer has the N-polarity determined by the HAADF analysis. The inversion domain boundary become smooth and flatter with the rising annealing temperature. The surface of MT-AlN buffer was finely rugged before the annealing, but became coarser and smoother with annealing. The changes in the surface morphology indicates the occurrence of grain coalescence. The density of TDs was reduced to roughly $5 \times 10^8 \text{ cm}^{-2}$ after annealing at $1650^\circ C$. Conclusively, this research confirms that pre-deposition and post deposition annealing are an effective treatment to control the microstructure and to reduce the dislocation density for advancement of semiconductor devices.

ABSTRAK

Prestasi peranti semikonduktor bergantung kuat kepada mikrostruktur bahan. Oleh itu kawalan mikrostruktur untuk mengurangkan ketumpatan kecacatan penting untuk fabrikasi peranti berprestasi tinggi. Dalam kajian ini, perubahan dan mekanisme mikrostruktur telah dianalisis secara terperinci. Lapisan nipis AlN telah di mendap atas substrat (0001) nilam dengan kaedah *metal organic vapor phase epitaxy (MOVPE)*, di mana proses pertumbuhan dalam cara yang agak konvensional, tetapi rawatan penyepuhlindapan ditambah sebelum dan selepas pemendapan. Kekasaran permukaan lapisan AlN telah diperhatikan dengan *atomic force microscope (AFM)*. Lapisan AlN diperhatikan dengan menggunakan mikroskop elektron penghantaran konvensional (CTEM) pada 200kV. Tinggi sudut anulus gelap-bidang (HAADF) imej imbasan-TEM juga diperhatikan dengan *scanning transmission electron microscope (STEM)* pada 300 kV. Penipisan spesimen untuk pemerhatian TEM telah dibuat menggunakan *focus ion beam (FIB)* dengan voltan dari 15kV ~ 3 kV. Sebelum pemendapan lapisan MT-AlN, substrat nilam itu disepuh lindap pada suhu yang tinggi dalam gas hydrogen, H₂. Pada suhu penyepuhlindapan, T_{an} <1250° C, penghabluran bertambah baik tetapi domain berpusing muncul. Kecacatan bebenang jenis c, jenis (a + c) dan berpusing domain dengan 200-500 nm diameter sepanjang [2-1-10], dengan kepadatan 10⁸ cm⁻² telah diperhatikan. Walau bagaimanapun apabila suhu telah meningkat kepada 1350°C kecacatan bebenang semakin berkurang justeru telah meningkatkan lekatan antara nilam dan AlN. Di samping itu, pemendapan penyepuhlindapan telah di jalankan pada suhu yang tinggi antara 1500°C untuk 1700°C untuk 2 jam di bawah suasana N₂ + CO. Keratan rentas TEM telah mendedahkan bahawa selepas penyepuhlindapan pada suhu 1500°C, domain berbentuk kon dan kecacatan bebenang kekal. Morfologi dan keadaan pembelauan untuk kontras imej sangat menyarankan bahawa domain adalah domain penyongsangan. Kecacatan bebenag jenis-a dan jenis-a + c dapat di lihat untuk g = 01-10 di bawah keadaan dua rasuk. Walau bagaimanapun, selepas penyepuhlindapan pada 1550°C, domain penyongsangan bersatu antara satu sama lain untuk meninggalkan sempadan domain berjalan secara zigzag di tengah-tengah lapisan AlN. Lapisan atas mempunyai kutub-Al dan lapisan yang lebih rendah mempunyai kutub-N. Sempadan domain penyongsangan menjadi semakin licin dengan suhu penyepuhlindapan yang semakin meningkat. Permukaan MT-AlN penampakan telah halus lasak sebelum penyepuhlindapan, tetapi menjadi lebih licin dengan penyepuhlindapan. Perubahan dalam morfologi permukaan menunjukkan berlakunya geseran sempadan domain. Ketumpatan TDS telah dikurangkan kepada kira-kira 5 × 10⁸ cm⁻² selepas penyepuhlindapan pada suhu 1650°C. Kesimpulan daripada penyelidikan ini telah sahkan bahawa pra pemendapan dan selepas pemendapan penyepuhlindapan telah menjadi rawatan yang amat berkesan bagi mengawal struktur mikro dan mengurangkan ketumpatan kecacatan bebenang untuk kemajuan dalam fabrikasi peranti semikonduktor berkualiti tinggi

TABLE OF CONTENTS

CHAPTER	TITLE	PAGE
	DECLARATION	ii
	DEDICATION	iii
	ACKNOWLEDGEMENT	iv
	ABSTRACT	v
	ABSTRAK	vi
	TABLE OF CONTENTS	vii
	LIST OF TABLES	x
	LIST OF FIGURES	xi
	LIST OF ABBREVIATIONS	xvii
	LIST OF SYMBOLS	xix
	LIST OF APPENDIX	xx
1	INTRODUCTION	1
	1.1 Introduction	1
	1.2 Motivation of Study	4
	1.3 Problem Statement	7
	1.4 Research Objectives	8
	1.5 Research Scope	9
	1.6 Significance to Knowledge	9
2	LITERATURE REVIEW	11
	2.1 Introduction	11
	2.2 Aluminium Nitride Crystal Structure and Properties	11
	2.3 Application of Aluminium Nitride	12
	2.4 Types of Defects in Nitride Semiconductors	17
	2.4.1 Point Defects	18

2.4.2	Linear Defects or Dislocations	19
2.4.3	Surface or Planar Defects	21
2.5	Growth Techniques	23
2.5.1	Molecular Beam Epitaxy (MBE)	24
2.5.2	Hydride Vapour Phase Epitaxy (HVPE)	25
2.6	Methods to Reduce Defects in Thin Films	26
2.6.1	Effects of Annealing on the Microstructure	27
2.6.2	Effects of AlN Buffer Layer	36
2.6.3	Effects of Doping	40
2.6.4	Epitaxial Lateral Overgrowth (ELO)	43
3	METHODOLOGY	45
3.1	Introduction	45
3.2	Approach	45
3.3	Growth Technique of AlN Epitaxialby MOVPE	47
3.4	Specimen Preparation	48
3.4.1	Pre annealing or Cleaning of Sapphire Substrate	49
3.4.2	Post Annealing AlN Buffer Layer	50
3.4.3	FIB Sample Preparation	52
3.5	Fundamentals of Transmission Electron Microscope (TEM)	62
3.6	Structure of TEM	65
3.6.1	Bright Field Image (BF)	66
3.6.2	Dark Field Image (DF)	67
3.7	Electron Diffraction and Scattering Using TEM	68
3.8	Electron Diffraction Theories	69
3.8.1	Bragg's Law	69
3.8.2	Two Beam Condition	70
3.9	Fundamentals of Scanning Electron Microscope	71
3.10	Microstructural Crystallographic Characterization	
	Techniques	74
3.10.1	Convergent Beam Electron Diffraction (CBED)	74
3.10.2	High Angle Annular Dark Field (HAADF) STEM	76
3.10.3	Electron Backscatter Diffraction (EBSD)	77

3.11 Analytic Techniques	78
4 RESULT AND DISCUSSION	80
4.1 Introduction	80
4.2 Atomic Force Microscopy Results for Pre Annealing Sapphire Substrate	81
4.3 Dependence of Microstructure in AlN Thin Films on the Pre Annealing Temperature for Sapphire Substrate	83
4.4 Atomic Force Microscopy Results for Post Deposition AlN Buffer Layer	85
4.5 X-ray Rocking Curves (XRC) for Full Widths at Half Maximum (FWHM)	88
4.6 TEM Micrographs of AlN Buffer Layer Annealed At Various Temperature	92
4.6.1 Specimen Annealed at 1500°C	92
4.6.2 Specimen Annealed at 1550°C	93
4.6.3 Specimen Annealed at 1600°C	95
4.6.4 Specimen Annealed at 1650°C	96
4.7 Determination of Inversion Domains Polarity	100
4.7.1 Complementary Contrast At Same Area	100
4.7.2 High Angle Annular Dark Field Image (HAADF) Scanning Transmission Electron Microscope (STEM)	101
4.7.3 Convergent Beam Electron Diffraction (CBED)	105
5 CONCLUSION AND RECOMMENDATIONS	108
5.1 Conclusions	108
5.2 Contribution of the Thesis	110
5.3 Recommendations for Future Works	111
REFERENCES	112
Appendix A	127

LIST OF TABLES

TABLE NO.	TITLE	PAGE
1.1	Lattice and thermal mismatches between nitride and sapphire	6
3.1	Growth parameters of HT-AlN with MT-AlN buffer layer on sapphire	50
3.2	Annealing of AlN buffer layer using N ₂ and CO gas mixture	51

LIST OF FIGURES

FIGURE NO.	TITLE	PAGE
1.1	Phenomena of electroluminescence to emit light in LED (Raguse & Sites, 2015)	2
1.2	Relationship of bandgap and wavelength(Taniyasu & Kasu, 2010)	3
1.3	Influence of semiconductor bandgap energy with photon emission (Narendran <i>et al.</i> , 2005)	4
1.4	Crystal structure and lattice constant of aluminium nitride (Berger, 1997)	5
2.1	AlN substrates for microelectronic applications (Pang <i>et al.</i> , 2005)	13
2.2	Typical structure of lateral field excited inclined AlN film TFBAR (Dubois & Muralt, 1999)	14
2.3	(a) LED structure, (b) top view of LED (S. Zhao <i>et al.</i> , 2015)	15
2.4	The effect of crystal plane on emission (S. Zhao <i>et al.</i> , 2015)	16
2.5	Classification of the types of lattice defects based on dimensionality	18
2.6	Illustration of the types of point defects (A.Kelly, 2012)	19
2.7	Determination of Burgers vector b (Kittel, 2005)	20
2.8	Difference between edge dislocation and screw dislocation (Bakke & Moraes, 2012)	21
2.9	Comparison of perfect crystal and stacking faulted crystal (Yu <i>et al.</i> , 2013)	23
2.10	Molecular beam epitaxy system (Gherasoiu <i>et al.</i> , 2004)	25
2.11	HVPE process (Richter <i>et al.</i> , 2005)	26

2.12	TEM observation of microstructural changes in AlN thin films bright field and dark field image of AlN thin film (a),(b) before annealing, (c),(d) after annealing (Tong et al., 2011)	28
2.13	Transmission measurements for AlN on sapphire (a) before annealing, (b) after annealing at 1300 °C for 30 minutes (Tong et al., 2011)	29
2.14	Average RMS roughness vs annealing temperature under N ₂ and vacuum atmosphere (Wang et al., 2014)	30
2.15	Cross-sectional TEM bright-field images of AlN thin films: (a) the as-grown and (b) annealed at 1000 °C (Liu et al., 2009)	31
2.16	Influence of AlN thickness on the intrinsic stress (Gillinger et al., 2015)	32
2.17	Difference in thermal expansion with increasing temperature (a) 400°C (b) 600°C, (c) 800°C and (d) 1000°C (Wei et al., 2007)	33
2.18	Residual stresses of ZnO films: (a) preheated at 350–450 °C and (b) annealed at 550°C–1000 °C (Wei et al., 2007)	34
2.19	(a–d) Surface morphology of the as-grown and annealed InAlN films (Afzal et al., 2015)	35
2.20	Growth model for GaN film on (0001) sapphire substrate (a) with (b) without AlN buffer layer (Akasaki et al., 1989)	37
2.21	SEM image of GaN film grown on sapphire (0001) (a) substrate with (b) without AlN buffer layer (Amano et al., 1988)	37
2.22	SEM images of the GaN epilayers grown on the AlN buffer layers of different growth temperatures: (a) 1050oC; (b) 1080oC; (c) 1100oC; and (d) 1120oC (Lu et al., 2004)	39
2.23	Optical transmittance spectra of ZnO:Al thin films as a function of annealing temperature (Kim & Tai, 2007)	41
2.24	Planar SEM micrographs of undoped and 5 mol% Al-doped ZnO thin films annealed at various temperatures from 450°C to 850°C, the scale bar is 500 nm (Kuo et al., 2006)	42

3.1	Flow chart of research process	46
3.2	(a) Horizontal MOVPE (b) Horizontal MOVPE reactor (Manasreh, 2000)	48
3.3	Standard growth process of AlN template	49
3.4	Growth sequence of AlN epitaxial	50
3.5	Annealing process in graphite resistance furnace (Miyake et al., 2016)	51
3.6	Illustration steps for AlN epitaxial growth	52
3.7	Cutting orientation of AlN template	53
3.8	Carbon coater	55
3.9	Specimen after carbon coating	55
3.10	Tilted view of specimen after undergoing slope cutting and etching	57
3.11	Needle lift-out lamella from sample	58
3.12	Lamella attached to TEM mesh before thinning process	59
3.13	Schematic diagram of the FIB lift-out technique (Lotnyk et al., 2015)	59
3.14	Specimen undergo thinning (a) Mid beam condition,(b) Fine beam condition (c) UFine beam condition, (d) Ufine tilted specimen	61
3.15	Thinning of specimen with beam current a) 15kV b) 10kV c) 5kV and d) 3kV	61
3.16	First TEM machine built in 1933	63
3.17	Transmission electron microscope model JEM 2000EX	64
3.18	Transmission electron microscope model JEM 2100	64
3.19	(a) Transmission electron structure, (b) TEM model 2100F	66
3.20	Bright field image formation	67
3.21	Dark field image formation	67
3.22	Interaction of electron with specimen	69
3.23	The Bragg's description of diffraction	70
3.24	Phenomena of two beam condition represented by the two dimensional pattern of direct and diffracted spot	71
3.25	SEM layout and structure (Todokoro & Ezumi, 1999)	72

3.26	Everhart-thornley detector for SE and solid state diode detector for BSE (JEOL)	73
3.27	Difference between astigmatized and stigmator corrected images (JEOL)	74
3.28	Accumulation of electron charge for non or semiconductive specimen (JEOL)	74
3.29	Difference between SAD and CBED diffraction(Vermaut, Ruterana, & Nouet, 1997)	75
4.1	AFM images of sapphire and HT-AlN with different annealing temperature	81
4.2	Variation in FWHM values of XRCs of HT-AlN with different annealing temperature	82
4.3	Appearance of grains with different twisting angles	83
4.4	(a) (b) (c) TEM results for AlN specimens annealed at 1350°C, (d) (e) (f) specimens annealed at 1250°C	84
4.5	SEM images (a) out lens (b) in-lens (c) GROD annealed at 1350°C, SEM(d) out lens (e) in-lens (f) GROD annealed at 1250°C	85
4.6	AFM images of AlN buffer layers with various thicknesses grown at $T_{Buf} = 1150\text{ }^{\circ}\text{C}$ (a–c) before and (d–f) after annealing at $T_{An} = 1650\text{ }^{\circ}\text{C}$:(a, d) $t_{Buf} = 200\text{ nm}$, (b, e) $t_{Buf} = 300\text{ nm}$, and (c, f) $t_{Buf} = 1000\text{ nm}$	87
4.7	AFM images of the AlN buffer layers with $t_{Buf} = 300\text{ nm}$ grown at $T_{Buf} = 1150\text{ }^{\circ}\text{C}$ before and after annealing at $T_{An} = 1500\text{--}1750\text{ }^{\circ}\text{C}$	88
4.8	FWHMs of (0002)-plane XRCs for AlN buffer layers with various thicknesses grown at $T_{Buf} = 1150\text{ }^{\circ}\text{C}$ before and after annealing at $T_{An} = 1650\text{ }^{\circ}\text{C}$	89
4.9	FWHMs of (10-12)-plane XRCs for AlN buffer layers with various thicknesses grown at $T_{Buf} = 1150\text{ }^{\circ}\text{C}$ before and after annealing at $T_{An} = 1650\text{ }^{\circ}\text{C}$	90
4.10	FWHMs of (0002) plane XRCs for AlN buffer layers with $t_{Buf}=300\text{ nm}$ grown at $T_{Buf}=1150^{\circ}\text{C}$ after annealing at different temperatures	91

4.11	FWHMs of(10-12) –plane XRCs for AlN buffer layers with $t_{\text{Buf}}=300\text{nm}$ grown at $T_{\text{Buf}}=1150^\circ\text{C}$ after annealing at different temperatures	91
4.12	BF image and diffraction pattern with $g=0002$	93
4.13	DF image and schematic of dislocation with $g=0002$	93
4.14	DF image contrast with $g=01-10$ and diffraction pattern	93
4.15	Bright field image and schematic with $g=0002$	94
4.16	Dark field image and diffraction pattern taken under two beam condition with $g=01-10$	95
4.17	Bright field image and schematic of dislocation with $g=0002$	96
4.18	Dark field image and diffraction pattern with $g=0002$	96
4.19	Dark field image and diffraction pattern with $g=01-10$	96
4.20	BF image and schematic of dislocation taken at $g=0002$	98
4.21	DF image and diffraction pattern taken with $g=0002$	98
4.22	DF image and diffraction pattern taken with $g=01-10$	98
4.23	Changes of microstructure with high temperature annealing	99
4.24	(a) Dark-field cross-sectional TEM images of AlN template under the two-beam condition with (a) $g = 0002$ and (b) $g = 11-20$	100
4.25	Dark Field TEM image of specimen annealed at 1500°C with the same region one with (a) $g= (0002)$ and the other (b) with $g= (0002)$ have complimentary contrast	101
4.26	(a) Wurtzite crystal structure, (b) Projected structure at $2-1-10$	102
4.27	Expected image contrast for HAADF-STEM	103
4.28	HAADF-STEM image of an area containing boundary between the upper and lower layers	104
4.29	Enlarged HAADF-STEM image of extracted from the upper and lower layer	104
4.30	TEM image with CBED pattern by 120 kV accelerating voltage	106
4.31	TEM image with CBED pattern by 300 kV accelerating voltage	106

4.32	CBED patterns and difference in atomic number by simulation	107
------	---	-----

107

LIST OF ABBREVIATIONS

ALD	-	Atomic Layer Deposition
BSE	-	Backscatter Electron
BF	-	Bright Field
CBED	-	Convergent Beam Electron Diffraction
DF	-	Dark Field
EBS	-	Electron Back Scatter Diffraction
ELO	-	Epitaxial Lateral Overgrowth
FIB	-	Focused Ion Beam
FWHM	-	Full Width Height Maximum
HAADF	-	High Angle Annular Dark Field Image
HCP	-	Hexagonal Close Packet
HT	-	High temperature
HVPE	-	Hydride Vapor Phase Epitaxy
ID	-	Inversion Domain
LED	-	Light Emitting Diode
LD	-	Laser Diode
MBE	-	Molecular Beam Epitaxy
MOCVD	-	Metal Organic Chemical Vapor Deposition
MOVPE	-	Metal Organic Vapor Phase Epitaxy
PL	-	Photoluminescence
RMS	-	Root Mean Square
SAW	-	Surface Acoustic Wave
SAD	-	Selected Area Diffraction
SE	-	Secondary Electron
TD	-	Threading Dislocation
TDD	-	Threading Dislocation Density
TEM	-	Transmission Electron Microscope

UV LED	-	Ultra Violet Light Emitting Diode
XRD	-	X-Ray Diffraction

LIST OF SYMBOLS

λ	-	Wavelength of incident wave
d	-	Interplanar distance
h	-	Plank's constant
mv	-	Nonrelativistic electron momentum
$\sin \theta$	-	Scattering angle
$\langle uvw \rangle$	-	Components of Burgers vector
$ b $	-	Magnitude of Burger's vector

LIST OF APPENDIX

APPENDIX	TITLE	PAGE
A	List of Publications and Conferences	127

CHAPTER 1

INTRODUCTION

1.1 Introduction

Nowadays, everyone is already familiar with semiconductors based bright blue, green and red light emitting diodes (LEDs) that light up our electronic appliances, decorate our streets and illuminate airport runways. LEDs are built mostly based on nitride semiconductors such as aluminium nitride (AlN), gallium nitride (GaN), indium nitride (InN) and their alloying materials with wide wavelength ranging from the infrared to ultraviolet. In 1902, British scientist Henry J. Round discovered the physical effect of electroluminescence. Electroluminescence is an optical and electrical phenomenon whereby a material emits light in response to an electric current or an external electric field.

In 1962, the first visible spectrum LED light was produced by Nick Holonyak Jr. and was red in colour (Mukai *et al.*, 1998). As technology progressed in the 1970's, LEDs were used in applications such as calculators, digital watches and test devices. Since emitting blue light was a difficult task thus it took almost three decades to produce the first blue LED in 1971 using GaN by Jacques Pankove (Nakamura & Mukai, 1992). This is because in order to produce blue LED, it required the development of techniques for the growth of high-quality crystals as well as the ability to control p-doping of semiconductors with high bandgap to produce heterojunctions, which was achieved with gallium-nitride (GaN) (Nakamura & Krames, 2013).

LEDs consist of several layers which are p-type layers, n-type layers and active region between them. P-type layer has a large hole concentration, where else N-type contains majority electron carriers. Between them is an active layer or also known as the p-n junction to which the negative electrons and positive holes are driven when electric voltage is applied to the semiconductor. When electrons and holes meet, they recombine and light is emitted. This phenomenon is known as electroluminescence as shown in Figure 1.1 (Raguse & Sites, 2015).

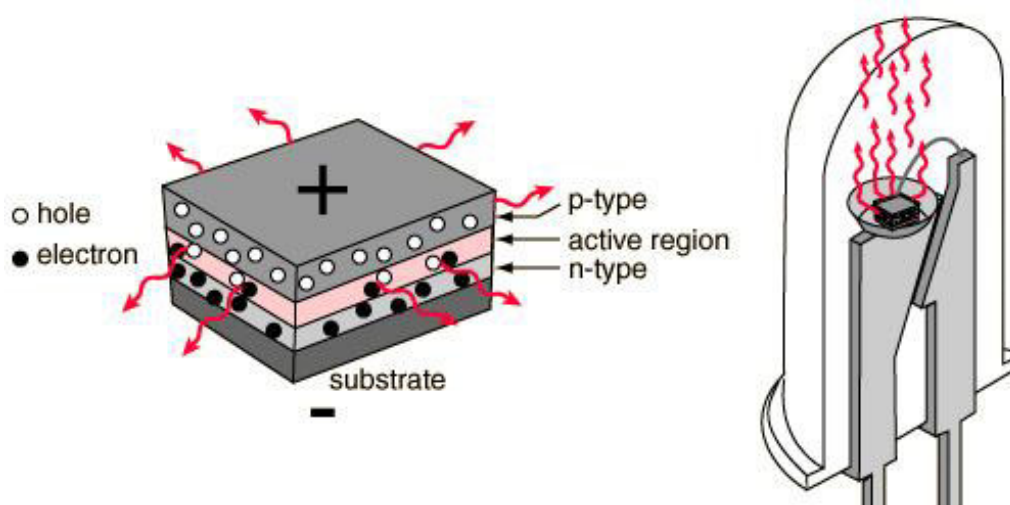


Figure 1.1 Phenomena of electroluminescence to emit light in LED (Raguse & Sites, 2015)

In order to have a good emission, it is essential to choose a suitable nitride semiconductor material which will emit light when electric current passed through it. Group III-V nitride semiconductors have been known for having outstanding optical, electronic and thermal properties. These materials have wurtzite or zinc blende crystal structures. AlN, GaN and AlGaIn have gained considerable attention as promising materials for optoelectronic devices in the blue and UV regions (Kuech, 2016; Manasreh, 2000). This is because these nitrides are semiconductor with wide band gap of direct transition for example, 3.4eV for GaN, 6eV for AlGaIn and 6.2eV for AlN at room temperature (Cardona & Kremer, 2014; Tripathy & Pattanaik, 2016).

Figure 1.2 shows the relationship between bandgap energy and wavelength of semiconductors. Light with wavelengths shorter than 400 nm is called ultraviolet

(UV) light. Since the emission wavelength is inversely proportional to the bandgap energy, a semiconductor with a wider bandgap emits light with a shorter wavelength. For instance, AlN has a wider direct- band gap energy of 6.3 eV and emits light with shorter wavelength, 210nm for deep ultraviolet UV LED.

On the other hand, the emission wavelength of GaN is 365nm with 3.2eV band gap energy and is used for high brightness blue LEDs and violet LDs for blue-ray equipment. Thus the wavelength of emitted light is determined by the bandgap energy of the semiconductor. Recently the winners of Noble prize physics, Akasaki's group of research invented the efficient blue LEDs using GaN, has led to white light sources for illumination. This light sources has long lifetime and requires ten times less energy than ordinary bulbs yet environmentally friendly (Akasaki &Amano, 2014).

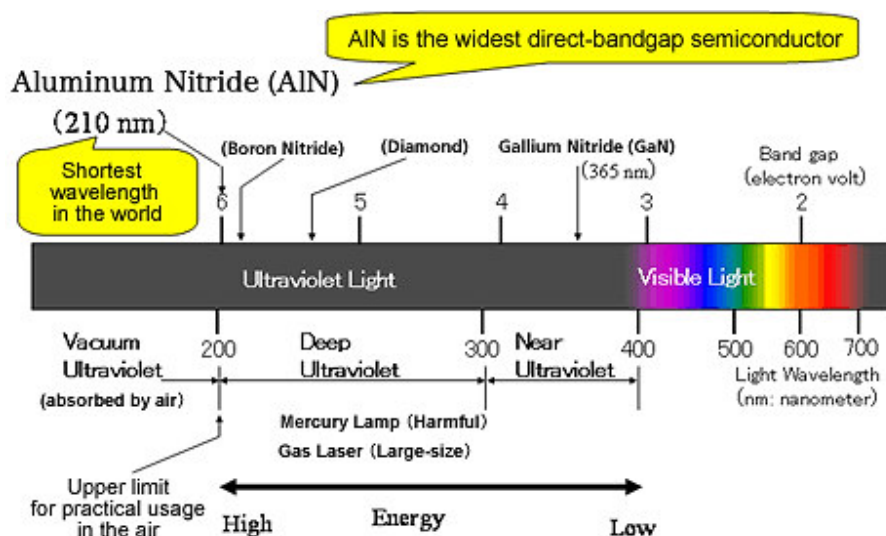


Figure 1.2 Relationship of bandgap and wavelength (Taniyasu & Kasu, 2010)

The definition of band gap is the energy needed to promote an electron from the lower energy valence band into the higher energy conduction band (Edwards, 2000). Hence, the wide band gap nitride semiconductor materials allows the devices to operate at much higher temperature, voltage and frequencies. The direct wide bandgap allows efficient absorption and emission of light. Due to this potential, semiconductor nitrides have been investigated to application for various optoelectronic devices, such as LED, Laser diodes (LD) and photo detectors for the

ultraviolet region. In complimentary with this, there is a significant relationship between the band gap energy and wavelength. In the process of recombination by emitting photons to produce light, the energy state of the electron hole- pair drops. However the emitted photon has a specific energy determined by the bandgap of the material making up the LED as shown in Figure 1.3 (Narendran *et al.*, 2005).

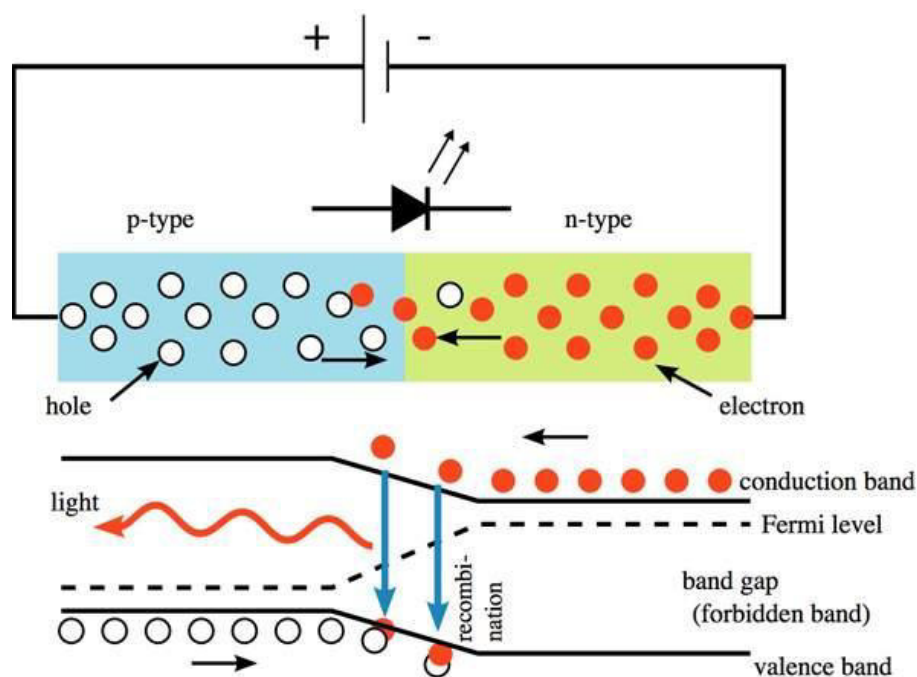


Figure 1.3 Influence of semiconductor bandgap energy with photon emission (Narendran *et al.*, 2005)

1.2 Motivation of Study

In this research, AlN was used as it stands out with the widest direct band gap among the III-V nitrides and that makes it a key component of deep-ultraviolet light source and detection. Due to its high acoustic velocity and strong piezoelectricity, AlN is also used in the application of surface acoustic wave devices (SAW). AlN is thermally stable at high temperature with high thermal conductivity as well as high dielectric strength which promotes it to be used in high power electronic devices. In conjunction with the characteristics of conducting electricity in extreme

environments, AlN demonstrates significantly higher performance while demanding less power.

AlN crystallizes in the wurtzite structure with lattice constants of $a=3.111 \text{ \AA}$ and $c=4.978 \text{ \AA}$ under the space group P63mc hexagonal as shown in Figure 1.4. AlN is stable at high temperature in inert atmosphere and it melts at 2800°C . It starts to decompose at 1400°C under the ambient atmosphere which makes it suitable for the usage at high temperature for heat treatment or annealing (Berger, 1997). However, the ultimate performance of AlN is limited by lattice defects that reduce its efficiency. In addition, it is very difficult to grow high quality epitaxial layer of AlN, and several issues such as a high defect density and piezoelectricity still remain to be resolved in thin-film growth process. Globally, researchers have made a number of attempts in growing crystals including single crystals of high quality on substrates such as silicon carbide (SiC) and sapphire (Al_2O_3).

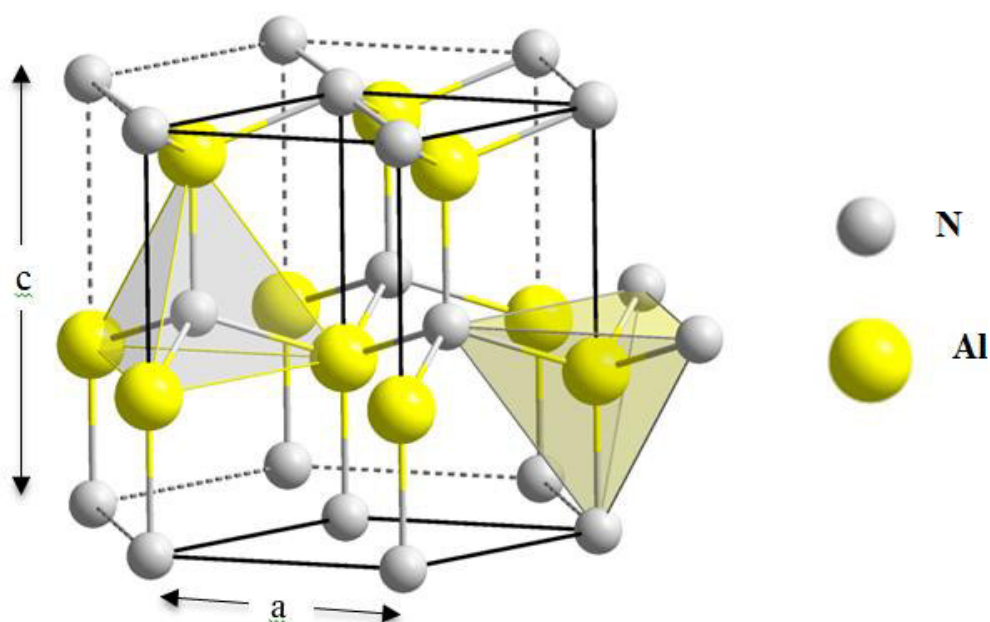


Figure 1.4 Crystal structure and lattice constant of aluminium nitride (Berger, 1997)

Various methods have been reported recently on the growth of nitride semiconductor thin films including hydride vapor phase epitaxy (HVPE), molecular beam epitaxy (MBE) and metal organic vapor phase epitaxy (MOVPE) using sapphire as a substrate (Ishida *et al.*, 2000; S. Wang *et al.*, 2015; W. Wang *et al.*,

2016; Yang *et al.*, 2015). However it has been difficult to grow high quality heteroepitaxial layer especially with a smooth top surface without cracks and other defects. This is because of the large lattice mismatch and large difference in thermal expansion coefficient between the nitride films and sapphire substrate. Table 1.1 shows the lattice constants and thermal expansion coefficient differences of AlN and GaN with sapphire substrate.

Table 1.1 : Lattice and thermal mismatches between nitride and sapphire

Elements	Lattice constant (Å)	Thermal expansion coefficient x 10⁻⁶(K⁻¹)
GaN	a = 3.189	5.59
	c = 5.182	7.75
AlN	a = 3.111	5.3
	c = 4.980	4.2
Sapphire	a = 4.758	7.5
	c = 12.991	8.5

The large lattice mismatch between AlN and sapphire resulted to 13% leads to dislocation defects in the AlN epitaxial. (Dovidenko *et al.*, 1996). A certain lattice mismatch is currently unavoidable but a reduction of threading dislocation (TDs) is required. Thus in order to reduce TDs, initially the growth parameters and steps should be modified. Complimentary to this, thin buffer layers also results in reduction of these defects. Recent development has succeeded in improving remarkably the surface morphology as well as the electrical and optical properties of AlN, GaN and AlGaIn alloy films by preceding deposition of a thin AlN layer as a buffer layer (Ito *et al.*, 1999; Xiong *et al.*, 2013). Mainly AlN is used as a buffer layer because Al is hard and it bends the dislocation to prevent it to reach the surface of the nitride semiconductor therefore reduces the density of dislocation (Kuwano *et al.*, 2010). This phenomena will be further explained in the next chapter. As for AlGaIn/GaN systems, GaN layer thickness is increased to reduce the dislocation density (Akasaki *et al.*, 1989).

In conjunction with this, a model for the growth process of high quality crystals whereby the crystallographic quality is examined using scanning electron microscope (SEM), reflection high energy electron diffraction (RHEED) and X-ray Diffraction (XRD). However usage of Transmission Electron Microscope (TEM) to clarify the microstructure inside the nitride semiconductors epitaxial films are not many. Nevertheless, cross sectional TEM observation of AlN grown on sapphire substrate is essential to provide detailed information. This is to control the microstructure and growth process of thin films including formation and annihilation process of defects for further analysis and characterization of nitride semiconductors. There are many other methods to reduce dislocations such as deposition of buffer layers, doping and epitaxial lateral overgrowth which will all be described in the next chapter. Annealing at high temperature is the method chosen by author and shall be discussed in detail. Annealing is a heat treatment process on the material which alters the materials microstructure by causing changes in physical, electrochemical and piezoelectric properties.

1.3 Problem Statement

When a thin film of AlN is grown or deposited on a sapphire substrate which has a large lattice mismatch and the large difference in the thermal expansion, it usually contains many structural defects. The density of dislocation is high normally in the range of 10^{10}cm^{-2} . Besides threading dislocations, there are many other kinds of structural defects, such as inversion domain, stacking mismatch boundaries, voids, and stacking faults. These defects disrupts the periodicity of the crystal over the length of several atomic diameters thus degrades the optoelectronic properties. For instance, a threading dislocation acts as a nonradiative and scattering center in electron transport which effects the performance of LEDs and field effect transistor.

In addition, the inefficiency of optoelectronic devices are also caused by dislocations defects as rapid nonradiative recombination of holes without conversion of their available energy into photon causes heating up of the crystal. This leads to the deterioration of emission efficiency. Other than that optoelectronic devices have

a shorter lifetime compared to devices with fewer defects. Thus the core problem is the inefficiency of devices due to defects in the material.

To my best knowledge, there is a lack of research conducted to characterize and analyze the lattice defects in details by transmission electron microscopy (TEM) although information obtained would be very useful in improving existing devices. This may be because very high skills and diffraction knowledge is required for one to characterize using TEM. The specimen preparation method is also very crucial and tedious. Moving on from here onwards, it is important to identify the right parameters which can assist to reduce lattice defects so that a high quality epitaxial film can be obtained. Many researchers have reported various ways to reduce the lattice defects, however a realistic condition in growing thin films without any defects have not be established yet. Annealing is one of the method which can reduce lattice defects in the epitaxial layer and has been employed by author before and after deposition of epitaxial layer.

Author studied the changes in microstructure due to high temperature annealing of AlN epitaxial on sapphire substrate. The core problem need to be identified at an early stage of the growth process to reduce or avoid defects in the crystal. Hence, this research aims to identify, analyse and characterize the defects in order to reduce the dislocation thus producing high quality thin films. The growth process of thin films with different parameters and conditions is also discussed in detail.

1.4 Research Objectives

The objective of this research is to determine the annealing effects in AlN epitaxial layer by:

- i. Characterizing and analysing the defects in AlN thin film grown on sapphire substrate using TEM

- ii. Identifying the changes of microstructure in AlN thin film after pre and post annealing treatment
- iii. Determining the polarity of AlN thin film to categorize the defect type
- iv. Establishing the growth parameters for higher quality AlN thin film.

1.5 Research Scope

This research was conducted in collaboration with the research groups of Mie University, Japan whereby the growth of AlN epitaxial on sapphire substrate using metalorganic vapour phase epitaxy (MOVPE) was carried out there. Annealing treatment was induced before and after the deposition of AlN buffer layer. The specimen provided by collaborators were further examined by author using electron microscopy technique at the facility of Kyushu University, Japan. After the formation process of lattice defects in the epitaxial were clarified, remedies for the condition to grow high quality thin films were proposed for establishment of the crystal growth. Especially the effects of heat treatments or annealing on the microstructure were investigated in details by using sophisticated TEM techniques.

The results of the research are important as to establish and improvise the parameters in growth conditions. In short, this research focuses on how does high temperature annealing can reduce the lattice defects in aluminium nitride thin films, thus is used for fabrication of high quality semiconductor devices.

1.6 Significance to Knowledge

The contribution of this study is to provide information to fellow researchers on the effects of annealing treatment in order to reduce the dislocation density in the AlN epitaxial layer by advanced TEM techniques. The crystallographic polarity determination also contributes to the identification of inversion domains in optoelectronic applications. Not only that, the annihilation mechanism of aluminium nitride heteroepitaxial layers lattice defects are also very useful. Furthermore, the

growth conditions plays an important role thus the establishment is crucial too. This research also focuses on the development of high quality nitride semiconductor epitaxial using combinations of alloys and AlN buffer layers. By reducing the defects in the AlN epitaxial, the semiconductor based devices performance can be improved, which leads to saving cost and reduce energy consumption. In addition the reduction of defects also improves the optical, chemical and piezoelectric properties of the optoelectronic devices.

REFERENCES

- Adachi, M., Takasugi, M., Morikawa, D., Tsuda, K., Tanaka, A., & Fukuyama, H. (2012). Analysis of the dislocation and polarity in an AlN layer grown using Ga-Al flux. *Applied Physics Express*, 5(10), 18–21. <http://doi.org/10.1143/APEX.5.101001>
- Afzal, N., Devarajan, M., & Ibrahim, K. (2015). Post-deposition annealing of magnetron sputtered InAlN film at different temperatures. *Journal of Alloys and Compounds*, 640, 260–266. <http://doi.org/10.1016/j.jallcom.2015.04.014>
- Akasaki, I., Amano, H., Koide, Y., Hiramatsu, K., & Sawaki, N. (1989). Effects of an buffer layer on crystallographic structure and on electrical and optical properties of GaN and Ga_{1-x}Al_xN (0 < x ≤ 0.4) films grown on sapphire substrate by MOVPE. *Journal of Crystal Growth*, 98(1-2), 209–219. [http://doi.org/10.1016/0022-0248\(89\)90200-5](http://doi.org/10.1016/0022-0248(89)90200-5)
- Akasaki, I., H.Amano, S. N. (2014). Metalorganic Vapor Phase Epitaxial Growth of Nonpolar Al(Ga,In)N Films on Lattice-Mismatched Substrates. In *Nobel prizes 2014* (Vol. 53). <http://doi.org/10.1002/annie.210409871>
- Akira, U., Haruo, S., Akira, S., & Yamaguchi, A. A. (1997). Thick GaN Epitaxial Growth with Low Dislocation Density by Hydride Vapor Phase Epitaxy. *Japanese Journal of Applied Physics*, 36(7B), L899. <http://doi.org/10.1143/JJAP.36.L899>
- Amano, H., Akasaki, I., Hiramatsu, K., Koide, N., & Sawaki, N. (1988). Effects of the buffer layer in metalorganic vapour phase epitaxy of GaN on sapphire substrate. *Thin Solid Films*, 163, 415–420. [http://doi.org/10.1016/0040-6090\(88\)90458-0](http://doi.org/10.1016/0040-6090(88)90458-0)
- Amano, H., N. Sawaki, I. A. and Y. T. (1986). Metalorganic vapor phase epitaxial growth of a high quality GaN film using an AlN buffer layer. *Appl. Phys. Lett*, 48(353).
- Assouar, M. B., El Hakiki, M., Elmazria, O., Alnot, P., & Tiusan, C. (2004).

- Synthesis and microstructural characterisation of reactive RF magnetron sputtering AlN films for surface acoustic wave filters. *Diamond and Related Materials*, 13(4-8), 1111–1115. <http://doi.org/10.1016/j.diamond.2003.11.064>
- Bakke, K., & Moraes, F. (2012). Threading dislocation densities in semiconductor crystals: A geometric approach. *Physics Letters A*, 376(45), 2838–2841. <http://doi.org/10.1016/j.physleta.2012.09.006>
- Berger, I., L. (1997). *Semiconductor materials* (1st ed.). CRC Press.
- Biswas, M. (n.d.). Impact of annealing temperature on structural, electrical and optical properties of epitaxial GaN thin films grown on sapphire substrates by PA-MBE, (0001).
- Callister, W.D., D. . R. (2000). *Fundamentals of Material Science and Engineering* (4th ed.). John Wiley and Sons Inc.
- Cao, B., Wang, P., & Gan, Z. (2016). Enhanced wall-plug efficiency in diodes with uniform current spreading p -electrode structures. *Journal of Applied Physics*, 49(235101). <http://doi.org/10.1088/0022-3727/49/23/235101>
- Cardona, M., & Kremer, R. K. (2014). Temperature dependence of the electronic gaps of semiconductors. *Thin Solid Films*, 571(P3), 680–683. <http://doi.org/10.1016/j.tsf.2013.10.157>
- Character, P., & Jul, N. (2016). The Reflection of X-rays by Crystals Author (s): W . H . Bragg and W . L . Bragg Source : Proceedings of the Royal Society of London . Series A , Containing Papers of a Published by : Royal Society Stable URL : <http://www.jstor.org/stable/93501> Accessed, 88(605), 428–438.
- Chu, S.-Y., Water, W., & Liaw, J.-T. (2003). Influence of postdeposition annealing on the properties of ZnO films prepared by RF magnetron sputtering. *Journal of the European Ceramic Society*, 23(10), 1593–1598. [http://doi.org/10.1016/S0955-2219\(02\)00404-1](http://doi.org/10.1016/S0955-2219(02)00404-1)
- David B. Williams, C. B. C. (2009). *Transmission Electron Microscope*. Springer.
- Dovidenko, K., S. Oktyabrsky, J. N. and M. R. (1996). Aluminum nitride films on different orientations of sapphire and silicon. *Appl. Phys. Lett.*, 79, 2439.
- Dubois, M.-A., & Muralt, P. (1999). Properties of aluminum nitride thin films for piezoelectric transducers and microwave filter applications. *Applied Physics Letters*, 74(20), 3032. <http://doi.org/10.1063/1.124055>
- Edwards, J., Kawabe, K., Stevens, G., & Tredgold, R. H. (1965). Space charge conduction and electrical behaviour of aluminium nitride single crystals.

- Solid State Communications*, 3(5), 99–100. [http://doi.org/10.1016/0038-1098\(65\)90231-0](http://doi.org/10.1016/0038-1098(65)90231-0)
- Edwards, N. V. (2000). *Residual stress in III-V nitrides. III-Nitride Semiconductors: Electrical, Structural and Defects Properties*. Woodhead Publishing Limited. <http://doi.org/10.1016/B978-044450630-6/50010-6>
- Evans, B. D., Pogatshnik, G. J., & Chen, Y. (2008). Optical properties of lattice defects in Al_xO_y , *91*(1994), 258–262.
- Ezumi, M., & Todokoro, H. (1997). Scanning electron microscope. *US Patent 5,608,218*.
- Floro, J. A., Hearne, S. J., Hunter, J. A., Kotula, P., Chason, E., Seel, S. C., & Thompson, C. V. (2001). The dynamic competition between stress generation and relaxation mechanisms during coalescence of Volmer–Weber thin films. *Journal of Applied Physics*, 89(9), 4886. <http://doi.org/10.1063/1.1352563>
- Gherasoiu, I., Nikishin, S., Kipshidze, G., Borisov, B., Chandolu, A., Ramkumar, C., ... Temkin, H. (2004). Growth mechanism of AlN by metal-organic molecular beam epitaxy. *Journal of Applied Physics*, 96(11), 6272–6276. <http://doi.org/10.1063/1.1813623>
- Giannuzzi, L. A., & Stevie, F. A. (1999). A review of focused ion beam milling techniques for TEM specimen preparation. *Micron*, 30(3), 197–204. [http://doi.org/10.1016/S0968-4328\(99\)00005-0](http://doi.org/10.1016/S0968-4328(99)00005-0)
- Gillinger, M., Schneider, M., Bittner, A., Nicolay, P., Schmid, U., Gillinger, M., ... Schmid, U. (2015). Impact of annealing temperature on the mechanical and electrical properties of sputtered aluminum nitride thin films Impact of annealing temperature on the mechanical and electrical properties of sputtered aluminum nitride thin films, 065303. <http://doi.org/10.1063/1.4907208>
- Goldstein, A. P., Andrews, S. C., Berger, R. F., Radmilovic, V. R., Neaton, J. B., & Yang, P. (2013). Zigzag inversion domain boundaries in indium zinc oxide-based nanowires: Structure and formation. *ACS Nano*, 7(12), 10747–10751. <http://doi.org/10.1021/nn403836d>
- Hemmingsson, C., Paskov, P. P., Pozina, G., Heuken, M., Schineller, B., & Monemar, B. (2007). Hydride vapour phase epitaxy growth and characterization of thick GaN using a vertical HVPE reactor. *Journal of Crystal Growth*, 300(1), 32–36. <http://doi.org/10.1016/j.jcrysgro.2006.10.223>

- Hideo Todokoro, T., & Makoto Ezumi, M. (1999). Scanning electron microscope, 13.
- Hiramatsu, K., Itoh, S., Amano, H., & Akasaki, I. (1991). Growth mechanism of GaN grown on sapphire with AlN buffer layer by MOVPE, 115.
- Hiramatsu, K., Nishiyama, K., Onishi, M., Mizutani, H., Narukawa, M., Motogaito, A., ... Maeda, T. (2000). Fabrication and characterization of low defect density GaN using facet-controlled epitaxial lateral overgrowth (FACELO). *Journal of Crystal Growth*, 221(1-4), 316–326. [http://doi.org/10.1016/S0022-0248\(00\)00707-7](http://doi.org/10.1016/S0022-0248(00)00707-7)
- Hirayama, H., Fujikawa, S., Norimatsu, J., Takano, T., Tsubaki, K., & Kamata, N. (2009). Fabrication of a low threading dislocation density ELO-AlN template for application to deep-UV LEDs. *Physica Status Solidi (C) Current Topics in Solid State Physics*, 6(SUPPL. 2), 2–5. <http://doi.org/10.1002/pssc.200880958>
- Hiroiyuki Fukuyama, Shin-ya Kusunoki, A. H. and K. H. (2006). Single crystalline aluminum nitride films fabricated by nitriding α -Al₂O₃. *Appl. Phys. Lett.*, 100.
- Hiroiyuki Fukuyama¹, a), Katsuhito Nakamura¹, Toshiaki Aikawa¹, Hidekazu Kobatake¹, Akira Hakomori², Kazuya Takada², and K. H. (2010). Nitridation behavior of sapphire using a carbon-saturated N₂-CON₂-CO gas mixture. *Journal of Applied Physics*, 107.
- Iborra, E.Olivares, J.Clement, M.Vergara, L.Sanz Hervás, A.Sangrador, J. (2004). Piezoelectric properties and residual stress of sputtered AlN thin films for MEMS applications. *Sensors and Actuators, A: Physical*, 115(2-3 SPEC. ISS.), 501–507. <http://doi.org/10.1016/j.sna.2004.03.053>
- Iwamoto, C., X. Q. Shen, H. Okumura, H. Matsuhata, Y. I. (2003). Termination mechanism of inversion domains by stacking faults in GaN. *Appl. Phys. Lett.*, 93, 3264.
- Inoue, S. I., Naoki, T., Kinoshita, T., Obata, T., & Yanagi, H. (2015). Light extraction enhancement of 265 nm deep-ultraviolet light-emitting diodes with over 90 mW output power via an AlN hybrid nanostructure. *Applied Physics Letters*, 106(13), 1–5. <http://doi.org/10.1063/1.4915255>
- Ishida, M., Ogawa, M., Orita, K., Imafuji, O., Yuri, M., Sugino, T., & Itoh, K. (2000). Drastic reduction of threading dislocation in GaN regrown on grooved stripe structure. *Journal of Crystal Growth*, 221(1-4), 345–349.

[http://doi.org/10.1016/S0022-0248\(00\)00711-9](http://doi.org/10.1016/S0022-0248(00)00711-9)

- Ito, T., Ohtsuka, K., Kuwahara, K., Sumiya, M., Takano, Y., & Fuke, S. (1999). Effect of AlN buffer layer deposition conditions on the properties of GaN layer. *Journal of Crystal Growth*, 205(1), 20–24. [http://doi.org/10.1016/S0022-0248\(99\)00241-9](http://doi.org/10.1016/S0022-0248(99)00241-9)
- Jakkaraju, R., Henn, G., Shearer, C., Harris, M., Rimmer, N., & Rich, P. (2003). Integrated approach to electrode and AlN depositions for bulk acoustic wave (BAW) devices. *Microelectronic Engineering*, 70(2-4), 566–570. [http://doi.org/10.1016/S0167-9317\(03\)00386-1](http://doi.org/10.1016/S0167-9317(03)00386-1)
- Jastrzebski, L., J.F. Corboy, R. S. (1989). Issues and Problems Involved in Selective Epitaxial Growth of Silicon for SOI Fabrication. *Journal of Electrochemical Society*, (136).
- Jang, K., Lee, K., Kim, J., Hwang, S., Lee, J., Dhungel, S. K., ... Å, J. Y. (2006). Effect of rapid thermal annealing of sputtered aluminium nitride film in an oxygen ambient, 9, 1137–1141. <http://doi.org/10.1016/j.mssp.2006.10.052>
- Jesbains Kaur, Noriyuki Kuwano, Khairur Rijal Jamaludin, Masatoshi Mitsuhashi, H. S., & Satoshi Hata, Shuhei Suzuki, Hideto Miyake, Kazumasa Hiramatsu, and H. F. (2016). Electron microscopy analysis of microstructure of postannealed aluminum nitride template. *Applied Physics Express*, 065502(9), 8–12. <http://doi.org/10.7567/APEX.9.065502>
- Johnson, M., Yu, Z., Brown, J., El-Masry, N., Cook, J., & Schetzina, J. (1999). Scanning electron microscopy and cathodoluminescence study of the epitaxial lateral overgrowth (ELO) process for gallium nitride. *Journal of Electronic Materials*, 28(3), 295–300. <http://doi.org/10.1007/s11664-999-0030-1>
- Jiang, N., T. J. Eustis, J. Cai, F. A. Ponce, J. C. H. S. and J. S. (2002). Polarity determination by atomic location by channeling-enhanced microanalysis. *Applied Physics Letters*, 80, 389.
- Kamohara, T., Akiyama, M., Ueno, N., Nonaka, K., & Tateyama, H. (2005). Growth of highly c-axis-oriented aluminum nitride thin films on molybdenum electrodes using aluminum nitride interlayers. *Journal of Crystal Growth*, 275(3-4), 383–388. <http://doi.org/10.1016/j.jcrysgro.2004.12.014>
- Kazuyuki Tadatomo, Hiroaki Okagawa, Youichiro Ohuchi, Takashi Tsunekawa, Yoshiyuki Imada, M. K. and T. T. (2001). High Output Power InGaN

- Ultraviolet Light-Emitting Diodes Fabricated on Patterned Substrates Using Metalorganic Vapor Phase Epitaxy. *Japanese Journal of Applied Physics*, 40.
- Kelly A., K. . K. (2012). *crystallography and crystal defects*. John Wiley and Sons.
- Kida, Y., Shibata, T., Miyake, H., & Hiramatsu, K. (2003). Metalorganic Vapor Phase Epitaxy Growth and Study of Stress in AlGa_N Using Epitaxial AlN as Underlying Layer. *Japanese Journal of Applied Physics*. <http://doi.org/10.1143/JJAP.42.L572>
- Kim, Y.-S., & Tai, W.-P. (2007). Electrical and optical properties of Al-doped ZnO thin films by sol–gel process. *Applied Surface Science*, 253(11), 4911–4916. <http://doi.org/10.1016/j.apsusc.2006.10.068>
- Kittel, C. (2005). Introduction to solid state physics, 688. http://doi.org/10.1007/SpringerReference_83
- Kobayashi, N. P., Junko T. Kobayashi, Choi, W.-J., Daniel Dapkus, P., Zhang, X., & H. Rich, D. (1998). Growth of single crystal GaN on a Si substrate using oxidized AlAs as an intermediate layer. *Journal of Crystal Growth*, 189-190(December), 172–177. [http://doi.org/10.1016/S0022-0248\(98\)00221-8](http://doi.org/10.1016/S0022-0248(98)00221-8)
- Kuech, T. F. (2016). III-V compound semiconductors: Growth and structures. *Progress in Crystal Growth and Characterization of Materials*, 1–19. <http://doi.org/10.1016/j.pcrysgrow.2016.04.019>
- Kuo, S. Y., Chen, W. C., Lai, F. I., Cheng, C. P., Kuo, H. C., Wang, S. C., & Hsieh, W. F. (2006). Effects of doping concentration and annealing temperature on properties of highly-oriented Al-doped ZnO films. *Journal of Crystal Growth*, 287(1), 78–84. <http://doi.org/10.1016/j.jcrysgro.2005.10.047>
- Kushvaha, S. S., Pal, P., Shukla, A. K., Joshi, A. G., Gupta, G., Kumar, M., ... Haranath, D. (2014). Effect of growth temperature on defects in epitaxial GaN film grown by plasma assisted molecular beam epitaxy. *AIP Advances*, 4(2). <http://doi.org/10.1063/1.4866445>
- Kuwano, N., Ezaki, T., Kurogi, T., Miyake, H., & Hiramatsu, K. (2010). Formation mechanism of Al-depleted bands in MOVPE-AlGa_N layer on GaN template with trenches. *Physica Status Solidi (C) Current Topics in Solid State Physics*, 7(7-8), 2036–2039. <http://doi.org/10.1002/pssc.200983424>
- Lan, Y. C., Crimp, M. A., Zhang, J. M., & Yang, Z. (2009). CBED APPLICATION IN CRYSTALLOGRAPHIC STRUCTURAL DETERMINATION, 48824.
- Lentzen, M., Jahnen, B., Jia, C. L., Thust, A., Tillmann, K., & Urban, K. (2002).

- High-resolution imaging with an aberration-corrected transmission electron microscope. *Ultramicroscopy*, 92(3-4), 233–242.
[http://doi.org/10.1016/S0304-3991\(02\)00139-0](http://doi.org/10.1016/S0304-3991(02)00139-0)
- Liu, B., F.U.QM, W.U KM, L.(2008). Studies of the Growth Method and Properties of AlN Grown by RF-MBE. *Journal of Korean and Physical Society*, 52(1), 17–19.
- Liu, B., Gao, J., Wu, K. M., & Liu, C. (2009). Preparation and rapid thermal annealing of AlN thin films grown by molecular beam epitaxy. *Solid State Communications*, 149(17-18), 715–717.
<http://doi.org/10.1016/j.ssc.2009.02.008>
- Lotnyk, A., Poppitz, D., Ross, U., Gerlach, J. W., Frost, F., Bernütz, S., ... Rauschenbach, B. (2015). Focused high- and low-energy ion milling for TEM specimen preparation. *Microelectronics Reliability*, 55(9-10), 2119–2125.
<http://doi.org/10.1016/j.microrel.2015.07.005>
- Lu, Y., Liu, X., Wang, X., Lu, D.-C., Li, D., Han, X., ... Wang, Z. (2004). Influence of the growth temperature of the high-temperature AlN buffer on the properties of GaN grown on Si(111) substrate. *Journal of Crystal Growth*, 263(1-4), 4–11. <http://doi.org/10.1016/j.jcrysgro.2003.11.001>
- Manasreh, M. O. (2000). *Introduction to defects and structural properties of III-nitride semiconductors. III-Nitride Semiconductors: Electrical, Structural and Defects Properties*. Woodhead Publishing Limited.
<http://doi.org/10.1016/B978-044450630-6/50002-7>
- Marchand, H., L. Zhao, N. Zhang, B. Moran, R. Coffie, U.K. Mishra, J.S. Speck, S.P. Denbaars, J. A. F. (2001). Metalorganic chemical vapor deposition of GaN on Si(111): Stress control and application to field-effect transistors. *Journal of Applied Physics*, 89(7846).
- Meng, W.J., J. A. Sell, and T. A. P. (1994). Growth of aluminum nitride thin films on Si(111) and Si(001): Structural characteristics and development of intrinsic stresses. *Journal of Applied Physics*, 75(3446).
- Microscope, T. E. (2000). 6,111,253.
- Mitate, T., Sonoda, Y., & Kuwano, N. (2002). Polarity determination of wurtzite and zincblende structures by TEM. *Physica Status Solidi (A) Applied Research*, 192(2), 383–388.
[http://doi.org/10.1002/1521-396X\(200208\)192:2<383::AID-PSSA383>3.0.CO;2-A](http://doi.org/10.1002/1521-396X(200208)192:2<383::AID-PSSA383>3.0.CO;2-A)

- Miyagawa, R., Yang, S., Miyake, H., Hiramatsu, K., Kuwahara, T., Mitsuhashi, M., & Kuwano, N. (2012). Microstructure of AlN grown on a nucleation layer on a sapphire substrate. *Applied Physics Express*, 5(2). <http://doi.org/10.1143/APEX.5.025501>
- Miyake, H., Nishio, G., Suzuki, S., Hiramatsu, K., & Fukuyama, H. (2016). Growth of high-quality AlN on sapphire with a thermally annealed AlN buffer layer in N₂-CO. *Applied Physics Express*, 9(0002), 2–3.
- Motoaki Iwaya, Tetsuya Takeuchi, Shigeo Yamaguchi, Christian Wetzel, H. A. and I. A. (1998). Reduction of Etch Pit Density in Organometallic Vapor Phase Epitaxy-Grown GaN on Sapphire by Insertion of a Low-Temperature-Deposited Buffer Layer between High-Temperature-Grown GaN. *Japanese Journal of Applied Physics*, 37.
- Muramoto, Y., Kimura, M., & Nouda, S. (2014). Development and future of ultraviolet light-emitting diodes: UV-LED will replace the UV lamp. *Semiconductor Science and Technology*, 29(8), 084004. <http://doi.org/10.1088/0268-1242/29/8/084004>
- Nagashima, T., Hironaka, K., Ishizuki, M., Kumagai, Y., Koukitu, A., & Takada, K. (2009). Polarity control and preparation of AlN nano-islands by hydride vapor phase epitaxy. *Physica Status Solidi (C) Current Topics in Solid State Physics*, 6(SUPPL. 2), 444–446. <http://doi.org/10.1002/pssc.200880823>
- Nakamura, S., & Krames, M. R. (2013). History of gallium-nitride-based light-emitting diodes for illumination. *Proceedings of the IEEE*, 101(10), 2211–2220. <http://doi.org/10.1109/JPROC.2013.2274929>
- Nakamura, S., & Mukai, T. (1992). High-Quality InGaN Films Grown on GaN Films. *Jpn. J. Appl. Phys.*, 31(10B), L1457–L1459. <http://doi.org/10.1143/JJAP.31.L1457>
- Narendran, N., Gu, Y., Freyssinier-Nova, J. P., & Zhu, Y. (2005). Extracting phosphor-scattered photons to improve white LED efficiency. *Physica Status Solidi (A) Applications and Materials Science*, 202(6), 60–62. <http://doi.org/10.1002/pssa.200510015>
- Naresh-Kumar, G., Hourahine, B., Vilalta-Clemente, A., Ruterana, P., Gamarra, P., Lacam, C., ... Trager-Cowan, C. (2012). Imaging and identifying defects in nitride semiconductor thin films using a scanning electron microscope. *Physica Status Solidi (a)*, 209(3), 424–426.

<http://doi.org/10.1002/pssa.201100416>

- Nomura, T., Okumura, K., Miyake, H., Hiramatsu, K., Eryu, O., & Yamada, Y. (2012). AlN homoepitaxial growth on sublimation-AlN substrate by low-pressure HVPE. *Journal of Crystal Growth*, 350(1), 69–71. <http://doi.org/10.1016/j.jcrysgro.2011.12.025>
- Ok-Hyun Nam, Michael D. Bremser, T. S. Z. and R. F. D. (1997). Lateral epitaxy of low defect density GaN layers via organometallic vapor phase epitaxy. *Journal of Applied Physics Letters*, 71(2638).
- Okano, H., N.Tanaka, Y.Takahashi, T.Tanaka, K.Shibata, S. N. (1994). Preparation of aluminum nitride thin films by reactive sputtering and their applications to GHz - band surface acoustic wave devices. *Appl. Phys. Lett*, 64(166).
- Olivares, J., Iborra, E., Clement, M., Vergara, L., Sangrador, J., & Sanz-Hervás, A. (2005). Piezoelectric actuation of microbridges using AlN. *Sensors and Actuators, A: Physical*, 123-124, 590–595. <http://doi.org/10.1016/j.sna.2005.03.066>
- Pang, W., Zhang, H., Kim, J. J., Yu, H., & Kim, E. S. (2005). High Q single-mode high-tone bulk acoustic resonator integrated with surface-micromachined FBAR filter. *IEEE MTT-S International Microwave Symposium Digest, 2005(C)*, 413–416. <http://doi.org/10.1109/MWSYM.2005.1516616>
- Parish, G., Keller, S., Kozodoy, P., Ibbetson, J. P., Marchand, H., Fini, P. T., ... Tarsa, E. J. (1999). High-performance (Al,Ga)N-based solar-blind ultraviolet p-i-n detectors on laterally epitaxially overgrown GaN. *Applied Physics Letters*, 75(2), 247. <http://doi.org/10.1063/1.124337>
- Przybyla, R. J., Tang, H. Y., Shelton, S. E., Horsley, D. A., & Boser, B. E. (2014). 12.1 3D ultrasonic gesture recognition. *Digest of Technical Papers - IEEE International Solid-State Circuits Conference*, 57, 210–211. <http://doi.org/10.1109/ISSCC.2014.6757403>
- Raguse, J. M., & Sites, J. R. (2015). Correlation of Electroluminescence With CdTe Solar Cells. *IEEE Journal of Photonics*, 5(4), 1175–1178.
- Ras, M. A., May, D., Winkler, T., Michel, B., & Wunderle, S. R. B. (2014). Thermal Characterization of Highly Conductive Die Attach Materials, 2014, 3–9.
- Reyntjens, S., & Puers, R. (2001). A review of focused ion beam applications in microsystem technology. *Journal of Micromechanics and Microengineering*, 11(4), 287–300. <http://doi.org/10.1088/0960-1317/11/4/301>

- Rebeiz, G.M., (2003). *RF MEMS theory, design and technology*. John Wiley and Sons.
- Richter, E., Hennig, C., Weyers, M., Habel, F., Tsay, J. D., Liu, W. Y., ... Kaeppler, J. (2005). Reactor and growth process optimization for growth of thick GaN layers on sapphire substrates by HVPE. *Journal of Crystal Growth*, 277(1-4), 6–12. <http://doi.org/10.1016/j.jcrysgro.2004.12.169>
- Rinaldi, F. (2002). *Basics of Molecular Beam Epitaxy*, 31.
- Robert, W., Alto, P., City, U., Takada, H., Okada, T. K., Edition, S., ... Alto, P. (2003). (12) United States Patent, I(12).
- Ruvimov, S. (2000). *Defect engineering in III-nitrides epitaxial systems*. Science. Woodhead Publishing Limited. <http://doi.org/10.1016/B978-044450630-6/50004-0>
- Ryan G. Banal, Mitsuru Funato, Y. K. (2008). Initial nucleation of AlN grown directly on sapphire substrates by metal-organic vapor phase epitaxy. *Appl. Phys. Lett*, 92.
- Satoh, I., Arakawa, S., Tanizaki, K., Miyanaga, M., Sakurada, T., Yamamoto, Y., & Nakahata, H. (2010). Development of aluminum nitride single-crystal substrates. *SEI Technical Review*, (71), 78–82.
- Schaffer, M., Schaffer, B., & Ramasse, Q. (2012). Sample preparation for atomic-resolution STEM at low voltages by FIB. *Ultramicroscopy*, 114, 62–71. <http://doi.org/10.1016/j.ultramic.2012.01.005>
- Seel, S. C., Thompson, C. V., Hearne, S. J., & Floro, J. a. (2000). Tensile stress evolution during deposition of Volmer–Weber thin films. *Journal of Applied Physics*, 88(12), 7079. <http://doi.org/10.1063/1.1325379>
- Serneels, R., M. Snykers, P. Delavignette, R. Gevers, and S. A. (1973). Friedel's law in electron diffraction as applied to the study of domain structure in non-centrosymmetrical crystals. *Phys. Status Solidi B* 58, 277.
- Shan, F. K., & Yu, Y. S. (2004). Band gap energy of pure and Al-doped ZnO thin films. *Journal of the European Ceramic Society*, 24(6), 1869–1872. [http://doi.org/10.1016/S0955-2219\(03\)00490-4](http://doi.org/10.1016/S0955-2219(03)00490-4)
- Sheldon, B. W., Rajamani, A., Bhandari, A., Chason, E., Hong, S. K., & Beresford, R. (2005). Competition between tensile and compressive stress mechanisms during Volmer-Weber growth of aluminum nitride films. *Journal of Applied Physics*, 98(4), 1–9. <http://doi.org/10.1063/1.1994944>

- Shigetaka Tomiyaa, Masao Ikedaa, Shinji Tanakaa, Yuya Kanitania, T. O. and K. H. (2010). Structural Defects in GaN-based Materials and Their Relation to GaN-based Laser Diodes. In *Materials Science in Semiconductor Processing* (Vol. 1195).
- Smith, S. A., & Gehrke, T. (2001). (19) United States (12), 1(19).
- Solanki, A. K., Kashyap, A., Nautiyal, T., Auluck, S., & Kahn, M. A. (1995). Optical Properties of AlN. *Solid State Communications*, 94(12), 1009–1012. [http://doi.org/10.1016/0038-1098\(95\)00087-9](http://doi.org/10.1016/0038-1098(95)00087-9)
- Sowers A.T, J. A. Christman, M. D. Bremser, B. L. Ward, R. F. D. and R. J. N. (1997). Thin films of aluminum nitride and aluminum gallium nitride for cold cathode applications. *Appl. Phys. Lett.*, 71, 2289.
- Strittmatter, A., Bimberg, D., Krost, A., Bläsing, J., & Veit, P. (2000). Structural investigation of GaN layers grown on Si(1 1 1) substrates using a nitridated AlAs buffer layer. *Journal of Crystal Growth*, 221(1-4), 293–296. [http://doi.org/10.1016/S0022-0248\(00\)00702-8](http://doi.org/10.1016/S0022-0248(00)00702-8)
- Stirman, J.N., F. A. Ponce, A. Davlovksa, I. S. T. Tsong, D. J. Smith. (2000). Polarity determination and atomic arrangements at a GaN/SiC interface using high-resolution image matching. *Appl. Phys. Lett*, 76, 822.
- Sun, M. S., Zhang, J. C., Huang, J., Wang, J. F., & Xu, K. (2016). AlN thin film grown on different substrates by hydride vapor phase epitaxy. *Journal of Crystal Growth*, 436, 62–67. <http://doi.org/10.1016/j.jcrysgr.2015.11.040>
- Tadigadapa, S. (2010). Piezoelectric microelectromechanical systems - Challenges and opportunities. *Procedia Engineering*, 5, 468–471. <http://doi.org/10.1016/j.proeng.2010.09.148>
- Takeuchi, T., Amano, H., Hiramatsu, K., Sawaki, N., & Akasaki, I. (1991). Growth of Single Crystalline Gan Film on Si-Substrate Using 3C-Sic As an Intermediate Layer. *Journal of Crystal Growth*, 115(1-4), 634–638. [http://doi.org/10.1016/0022-0248\(91\)90817-O](http://doi.org/10.1016/0022-0248(91)90817-O)
- Tanaka, S., Iwai, S., & Aoyagi, Y. (1997). Reduction of the defect density in GaN films using ultra-thin AlN buffer layers on 6H-SiC, 170, 329–334.
- Taniguchi, M., Hao, G., Nakaya, K., & Inoue, S. (n.d.). Optimization of AlN substrate geometry for Diodes.
- Taniyasu, Y., & Kasu, M. (2010). Improved emission efficiency of 210-nm deep-ultraviolet aluminum nitride light-emitting diode. *NTT Technical Review*,

8(8).

- Tong, H., Deng, Z., Liu, Z., & Huang, C. (2011). Applied Surface Science Effects of post-annealing on structural , optical and electrical properties of Al-doped ZnO thin films. *Applied Surface Science*, 257(11), 4906–4911. <http://doi.org/10.1016/j.apsusc.2010.12.144>
- Tripathy, S. K., & Pattanaik, A. (2016). Optical and electronic properties of some binary semiconductors from energy gaps. *Optical Materials*, 53, 1–28. <http://doi.org/10.1016/j.optmat.2016.01.012>
- Tsao, J. Y. (2004). The World of Compound Semiconductors. *Analysis*, 1–191.
- Tseng, A. A. (2004). Recent developments in micromilling using focused ion beam technology. *Journal of Micromechanics and Microengineering*, 14, R15–R34. <http://doi.org/10.1088/0960-1317/14/4/r01>
- Utlaut, M. (2014). *Focused ion beams for nano-machining and imaging. Nanolithography: The art of fabricating nanoelectronic and nanophotonic devices and systems*. Woodhead Publishing Limited. <http://doi.org/10.1533/9780857098757.116>
- Vergara, L., Clement, M., Iborra, E., Sanz-Hervás, A., García López, J., Morilla, Y., Respaldiza, M. A. (2004). Influence of oxygen and argon on the crystal quality and piezoelectric response of AlN sputtered thin films. *Diamond and Related Materials*, 13(4-8), 839–842. <http://doi.org/10.1016/j.diamond.2003.10.063>
- Vergara, L., Olivares, J., Iborra, E., Clement, M., Sanz-Hervás, A., & Sangrador, J. (2006). Effect of rapid thermal annealing on the crystal quality and the piezoelectric response of polycrystalline AlN films. *Thin Solid Films*, 515(4), 1814–1818. <http://doi.org/10.1016/j.tsf.2006.07.002>.
- Vainshtein, B.K., (1964). *Structure Analysis by Electron Diffraction*. (O. Pergamon Press, Ed.).
- Vermaut, P., Ruterana, P., & Nouet, G. (1997). Polarity of epitaxial layers and (1210)prismatic defects in GaN and AlN grown on the (0001)Si surface of 6H-SiC. *Philosophical Magazine A*, 76(6), 1215–1234. <http://doi.org/10.1080/01418619708214224>
- Wang, J., Li, S. N., & Liu, J. B. (2015). Migrations of pentagon-heptagon defects in hexagonal boron nitride monolayer: The first-principles study. *Journal of Physical Chemistry A*, 119(15), 3621–3627.

- <http://doi.org/10.1021/acs.jpca.5b01308>
- Wang, S., Zhang, X., Zhu, M., Li, F., & Cui, Y. (2015). Crack-free Si-doped n-AlGa_N film grown on sapphire substrate with high-temperature AlN interlayer. *Optik*, *126*(23), 3698–3702. <http://doi.org/10.1016/j.ijleo.2015.08.218>
- Wang, W., Yang, W., Wang, H., Zhu, Y., Yang, M., Gao, J., & Li, G. (2016). A comparative study on the properties of c-plane and a-plane GaN epitaxial films grown on sapphire substrates by pulsed laser deposition. *Vacuum*, *128*, 158–165. <http://doi.org/10.1016/j.vacuum.2016.03.032>
- Wang, W.-Y., Jin, P., Liu, G.-P., Li, W., Liu, B., Liu, X.-F., & Wang, Z.-G. (2014). Effect of high-temperature annealing on AlN thin film grown by metalorganic chemical vapor deposition. *Chinese Physics B*, *23*(8), 087810. <http://doi.org/10.1088/1674-1056/23/8/087810>
- Wei, X. Q., Zhang, Z. G., Liu, M., Chen, C. S., Sun, G., Xue, C. S., ... Man, B. Y. (2007). Annealing effect on the microstructure and photoluminescence of ZnO thin films. *Materials Chemistry and Physics*, *101*(2-3), 285–290. <http://doi.org/10.1016/j.matchemphys.2006.05.005>
- Westwood, A. D., & Notis, M. R. (1991). Inversion Domain Boundaries in Aluminum Nitride. *Journal of American Ceramic Society*, *74*(6), 1226–1239.
- Williams, D. B. C. C. (2015). Transmission Electron Microscopy, *1*(October). <http://doi.org/10.1017/CBO9781107415324.004>
- Xiong, H., Dai, J. N., Hui, X., Fang, Y. Y., Tian, W., Fu, D. X., ... He, Y. (2013). Effects of the AlN buffer layer thickness on the properties of ZnO films grown on c-sapphire substrate by pulsed laser deposition. *Journal of Alloys and Compounds*, *554*, 104–109. <http://doi.org/10.1016/j.jallcom.2012.08.117>
- Y.Nakada, I. . A. (1998). GaN heteroepitaxial growth on silicon nitride buffer layers formed on Si (111) surfaces by plasma-assisted molecular beam epitaxyle. *Applied Physics Letters*, *827*(73).
- Yang, M., Lin, Z., Zhao, J., Wang, Y., Li, Z., Lv, Y., & Feng, Z. (2015). Influence of sapphire substrate thickness on the characteristics of AlGa_N/AlN/GaN heterostructure field-effect transistors. *Superlattices and Microstructures*, *85*, 43–49. <http://doi.org/10.1016/j.spmi.2015.05.020>
- Yang, J.W., C. J. Sun, Q. Chen, M. Z. Anwar, M. Asif Khan, S. A. Nikishin, G. A. Seryogin, A. V. Osinsky, L. C. (1996). High quality GaN–InGa_N

heterostructures grown on (111) silicon substrates. *Applied Physics Letters*, 69(3566).

- Yasutoshi Kawaguchi, Shingo Nambu, Hiroki Sone, Takumi Shibata, Hidetada Matsushima, Masahito Yamaguchi, Hideto Miyake¹, K. H. and N. S. (1998). Selective Area Growth of GaN Using Tungsten Mask by Metalorganic Vapor Phase Epitaxy. *Japanese Journal of Applied Physics*, 37.
- Yu, K. Y., Bufford, D., Chen, Y., Liu, Y., Wang, H., & Zhang, X. (2013). Basic criteria for formation of growth twins in high stacking fault energy metals. *Applied Physics Letters*, 103(18). <http://doi.org/10.1063/1.4826917>
- Zamir, S., Meyler, B., Zolotoyabko, E., & Salzman, J. (2000). The effect of AlN buffer layer on GaN grown on (111)-oriented Si substrates by MOCVD. *Journal of Crystal Growth*, 218, 181–190. [http://doi.org/10.1016/S0022-0248\(00\)00570-4](http://doi.org/10.1016/S0022-0248(00)00570-4)
- Zhang, B. S., Wu, M., Shen, X. M., Chen, J., Zhu, J. J., Liu, J. P., ... Yang, H. (2003). Influence of high-temperature AlN buffer thickness on the properties of GaN grown on Si(1 1 1). *Journal of Crystal Growth*, 258(1-2), 34–40. [http://doi.org/10.1016/S0022-0248\(03\)01416-7](http://doi.org/10.1016/S0022-0248(03)01416-7)
- Zhang, D. H., & Brodie, D. E. (1994). Effects of annealing ZnO films prepared by ion-beam-assisted reactive deposition. *Thin Solid Films*, 238, 95–100. [http://doi.org/10.1016/0040-6090\(94\)90655-6](http://doi.org/10.1016/0040-6090(94)90655-6)
- Zhao, D. G., Zhu, J. J., Liu, Z. S., Zhang, S. M., Yang, H., & Jiang, D. S. (2004). Surface morphology of AlN buffer layer and its effect on GaN growth by metalorganic chemical vapor deposition. *Applied Physics Letters*, 85(9), 1499–1501. <http://doi.org/10.1063/1.1784034>
- Zhao, Q., Feng, S., Zhu, Y., Xu, X., Zhang, X., Song, X., ... Yu, D. (2006). Annealing effects on the field emission properties of AlN nanorods. *Nanotechnology*, 17, S351–S354. <http://doi.org/10.1088/0957-4484/17/11/S20>
- Zhao, S., Connie, a T., Dastjerdi, M. H. T., Kong, X. H., Wang, Q., Djavid, M., ... Mi, Z. (2015). Aluminum nitride nanowire light emitting diodes: Breaking the fundamental bottleneck of deep ultraviolet light sources. *Scientific Reports*, 5, 8332. <http://doi.org/10.1038/srep08332>
- Zhou, Y. G., Xie, S. Y., Lu, W. F., & Zheng, Y. D. (2001). Growth of high quality GaN layers with AlN buffer on Si (1 1 1) substrates, 225, 150–154.

- Zhu, B. L., Zhao, X. Z., Su, F. H., Li, G. H., Wu, X. G., Wu, J., & Wu, R. (2010). Low temperature annealing effects on the structure and optical properties of ZnO films grown by pulsed laser deposition. *Vacuum*, 84(11), 1280–1286. <http://doi.org/10.1016/j.vacuum.2010.01.059>
- Zi-qiang, X., Hong, D., Yan, L., & Hang, C. (2006). Al-doping effects on structure, electrical and optical properties of c-axis-orientated ZnO:Al thin films. *Materials Science in Semiconductor Processing*, 9(1-3), 132–135. <http://doi.org/10.1016/j.mssp.2006.01.082>
- Zno, Q. É., Lee, G. H., Iwata, N., Kim, S. J., & Kimb, M. S. (2005). Special Issue Innovative Ceramics (I)' Photoluminescence of ZnO Fine Powders Synthesized by Sol – Gel Process Special Issue Innovative Ceramics (I)', 66(I), 64–66.
- Zytkiewicz, Z. R. (2002). Laterally overgrown structures as substrates for lattice mismatched epitaxy. *Thin Solid Films*, 412(1-2), 64–75. [http://doi.org/10.1016/S0040-6090\(02\)00315-2](http://doi.org/10.1016/S0040-6090(02)00315-2).